

# TC-Permitting GCM Simulations of Hurricane Frequency Response to Sea Surface Temperature Anomalies Projected for the Late-Twenty-First Century

MING ZHAO

*NOAA/Geophysical Fluid Dynamics Laboratory, Princeton, New Jersey, and University Corporation for Atmospheric Research, Boulder, Colorado*

ISAAC M. HELD

*NOAA/Geophysical Fluid Dynamics Laboratory, Princeton, New Jersey*

(Manuscript received 14 June 2011, in final form 19 September 2011)

## ABSTRACT

A tropical cyclone-permitting global atmospheric model is used to explore the hurricane frequency response to sea surface temperature (SST) anomalies generated by coupled models for the late-twenty-first century. Results are presented for SST anomalies averaged over 18 models as well as from 8 individual models. For each basin, there exists large intermodel spread in the magnitude and even the sign of the frequency response among the different SST projections. These sizable variations in response are explored to understand features of SST distributions that are important for the basin-wide hurricane responses. In the North Atlantic, the eastern Pacific, and the southern Indian basins, most (72%–86%) of the intermodel variance in storm frequency response can be explained by a simple relative SST index defined as a basin's storm development region SST minus the tropical mean SST. The explained variance is significantly lower in the South Pacific (48%) and much lower in the western Pacific basin (27%). Several atmospheric parameters are utilized to probe changes in tropical atmospheric circulation and thermodynamical properties relevant to storm genesis in the model. While all present strong correlation to storm response in some basins, a parameter-measuring tropospheric convective mass flux stands out as skillful in explaining the simulated differences for all basins. Globally, in addition to a modest reduction of total storm frequency, the simulations exhibit a small, but robust eastward and poleward migration of genesis frequency in both the North Pacific and the North Atlantic Oceans. This eastward migration of storms can also be explained by changes in convection.

## 1. Introduction

What controls the global number and distribution of tropical cyclones (TC) and how might these change with changing climate? The large range of spatial and temporary scales associated with the physical and dynamical processes of TC genesis makes simple theories difficult (e.g., Emanuel 2008; Dunkerton et al. 2009). Recent studies using global climate models (GCM) offer a promising approach toward answering these questions (e.g., Sugi et al. 2002; McDonald et al. 2005; Yoshimura et al. 2006; Oouchi et al. 2006; Chauvin et al. 2006; Bengtsson

et al. 2007; Gualdi et al. 2008; LaRow et al. 2008; Zhao et al. 2009, hereafter ZHLV; Sugi et al. 2009; Held and Zhao 2011; Murakami et al. 2012). See Knutson et al. (2010) for a recent review. Despite still relatively coarse spatial resolution (20–100 km), these new atmospheric GCMs (AGCMs) permit a direct simulation of the generation of TC-like vortices with tropical storm and hurricane strength. When forced by the observed sea surface temperature (SST) distribution the models have demonstrated their ability in reproducing many features of TC frequency variability for the past few decades during which reliable observational data are available (e.g., ZHLV). These include the global geographical distribution, seasonal cycle, and interannual variability as well as decadal trend of storm frequency for multiple ocean basins.

When forced by the greenhouse gas-warmed SSTs (as well as the corresponding increase of concentration of

---

*Corresponding author address:* Dr. Ming Zhao, NOAA/Geophysical Fluid Dynamics Laboratory, Princeton University, Forrestal Campus, 201 Forrestal Rd., Princeton, NJ 08540-6649.  
E-mail: ming.zhao@noaa.gov

atmospheric CO<sub>2</sub>) projected by the coupled climate models, these TC-permitting AGCMs generally produce a reduction of total global number of TCs with a shift of the intensity probability distribution toward higher intensities (e.g., Yoshimura et al. 2006; Oouchi et al. 2006; Bengtsson et al. 2007; ZHLV; Sugi et al. 2009; Held and Zhao 2011). Furthermore, when the total greenhouse gas effects are broken down into the effect of increasing SST with fixed CO<sub>2</sub> and the effect of increasing CO<sub>2</sub> with fixed SSTs, Yoshimura and Sugi (2005) and Held and Zhao (2011) find that a significant fraction of the reduction in globally averaged TC frequency is due to the effect of the CO<sub>2</sub> increase with fixed SSTs.

Compared to the response of global mean TC frequency, the regional change of TCs, especially those of hurricane or major hurricane intensity may be of more societal interest. ZHLV investigated basin-wide hurricane frequency response to four different SST anomalies generated by coupled models in the Third Coupled Model Intercomparison Project (CMIP3) archive (Meehl et al. 2007) for the late-twenty-first century based on the A1B scenario. The SST anomalies were obtained from single realizations of three models and from the ensemble mean for the simulations for 18 models.<sup>1</sup> ZHLV found that despite the robust reduction of global mean frequency, the response of hurricane frequency in individual basins differ among the simulations. In particular, the response of the North Atlantic hurricane frequency scales with a relative SST index, which measures the relative warming of tropical Atlantic SST with respect to other ocean basins, is consistent with Swanson (2008) and Vecchi et al. (2008).

To what extent does the concept of relative SST controlling TC frequency apply for other ocean basins? What are the atmospheric mechanisms that translate these SSTs into processes that directly control the response of basin-wide hurricane activity to global warming in other basins? In this study, we further explore these questions by pursuing six additional global warming experiments. The increased number (now a total of 10) of

warming experiments allows us to better define the uncertainty for future projections, and a sizable intermodel variation in storm response permits a better identification of the environmental factors that are important for storm genesis in the model. Five of the new experiments are analogous to those in ZHLV except using SST anomalies from additional coupled models.

While our initial model selections focused primarily on increasing the range of variation in the projected relative warming of SSTs in the North Atlantic, this set of models is also sufficient in representing the CMIP3 ensemble spread of relative SST in other ocean basins (as can be seen from Fig. B1 in appendix B). In addition to these coupled model projections, we have also performed a simple experiment with the control SST uniformly warmed by 2 K (hereafter P2K). In all cases, including P2K, we also double the concentration of CO<sub>2</sub> in the atmosphere, a change consistent with that imposed over the twenty-first century in the A1B experiments. A list of the SST warming anomalies including their ID numbers (0–9, used in figures), acronyms, and the descriptions of the corresponding modeling groups is provided in appendix A.

The model used in this study is identical to that utilized in ZHLV. It employs a finite-volume dynamical core with a cubed-sphere grid topology (Putman and Lin 2007). Each face of the cube comprises 180 × 180 grid points, resulting in grid size ranging from 43.5 to 61.6 km. The model has 32 vertical levels and uses a modified version of the moist convection scheme of Bretherton et al. (2004) for both shallow and deep convection. More details of the numerics and physics of this model are provided by ZHLV and the (Geophysical Fluid Dynamics Laboratory) GFDL Global Atmospheric Model Development Team (2004).

The storm detection and tracking algorithm is described by ZHLV. As in ZHLV, we focus on TCs with near-surface (lowest model level, 35 m) wind speed reaching hurricane intensity (33 m s<sup>-1</sup>). The term “hurricanes” is used here in all basins for convenience. The definition of the ocean basins and naming conventions (North Atlantic, eastern Pacific, western Pacific, northern Indian, southern Indian, and South Pacific) follows the International Best Track Archive for Climate Stewardship [IBTrACS; Knapp et al. (2010), <http://www.ncdc.noaa.gov/oa/ibtracs/>]. A storm is assigned to an ocean basin based on its genesis location (the first location identified by the TC detection and tracking algorithm).

As described in ZHLV, we first generate a control simulation by prescribing the climatological SSTs (seasonally varying with no interannual variability) using time-averaged (1982–2005) Hadley Centre Global Sea Ice and Sea Surface Temperature (HadISST) data (Rayner

---

<sup>1</sup> As described in ZHLV, we compute the multimodel ensemble mean SST anomaly by differencing the period 2081–2100 and the period 2001–20 from the A1B simulations in the CMIP3 archive. For each of the individual models, we use one realization (run 1 in the CMIP3 archive) to compute the 2001–2100 linear trend. The linear trend is then multiplied by 0.8 so that it is consistent in magnitude with the 80-yr period (2010–90) used for the multimodel ensemble mean. The use of a century-scale linear trend instead of the difference between the two end periods helps reduce the contribution of internal variability in the individual models since only one realization is used for each model. For the ensemble mean, it makes little difference whether one uses the difference or the trend.

TABLE 1. A comparison of annual count of hurricanes and TCs (values in parentheses) for each basin between the model control simulation and the IBTrACS observations (1982–2005).

Basin	CNTL	IBTrACS
North Atlantic	5.6 (12.0)	6.4 (11.8)
Eastern Pacific	9.6 (23.5)	9.8 (20.4)
Western Pacific	22.2 (36.5)	16.3 (34.3)
Northern Indian	2.1 (6.7)	1.2 (7.2)
Southern Indian	9.1 (20.7)	8.5 (19.0)
South Pacific	5.7 (13.7)	5.6 (13.0)

et al. 2003). Table 1 provides a comparison of annual count of hurricanes and TCs for each basin between the model control simulation and the IBTrACS observations for the period 1982–2005. Both the geographical distribution of the mean numbers and the seasonal cycle (see Fig. 5 in ZHLV) at each basin compare well with the IBTrACS observations.

For the global warming experiments, we add the SST warming anomalies (also seasonally varying with no interannual variability) projected by the coupled models to the climatological SSTs and double the concentration of CO<sub>2</sub> in the atmosphere. The control experiment was integrated for 20 years while most of the warming experiments were carried out for 10 years because of the constraint of computer time. We have selected a few warming experiments [ENSEMBLE, P2K, and the Geophysical Fluid Dynamics Laboratory Climate Model version 2.0 (GFDL-CM2.1)] for 20-yr integration to test for sensitivity to integration length. In general, we do not find substantial differences for basin-wide mean frequency between the 10- and 20-yr statistics. We use the 20-yr averages for the cases available in the results described below.

## 2. Results

The response of hurricane frequency in each of the six ocean basins is shown in Fig. 1. We show the fractional changes in annual count from all 10 warming experiments. The 90% confidence interval is also shown for each result in the figure, assuming normal distributions and considering each year as an independent sample. In the North Atlantic, five of the models produce a significant reduction with the two Hadley Centre models generating the largest diminishment [–51% for the third climate configuration of the Met Office Unified Model (HADCM3) and –84% for the Hadley Centre Global Environmental Model version 1 (HADGEM1)]. In contrast, the ECHAM5 model produces a modest increase (20%–25%) of hurricanes with the rest presenting small changes whose sign cannot be determined with high

confidence. If we consider all TCs (including all storms with near-surface wind speed greater than 17 m s<sup>–1</sup>), none of the models produce an increase, indicating that the increase in hurricanes in some of the models is due to the fact that the effect of the shift of the storm intensity distribution toward higher values exceeds the effect of the reduction in total number of TCs upon warming (Zhao and Held 2010). For hurricanes and for all TCs there exists a large intermodel spread (standard deviation of fractional changes of ~0.35) in the magnitude of the response to warming in the North Atlantic.

In the eastern Pacific, five of the models produce a significant increase with the two Hadley Centre models (HADCM3 and HADGEM1) producing the sharpest rise (~120%). Only one model (GFDL-CM2.1) produces a significant reduction (–34%) with the other three models generating relatively small and insignificant changes. There is a negative correlation ( $r = -0.58$ ) between the response of hurricanes in the eastern Pacific and that in the North Atlantic among the simulations. All of the five models producing declining hurricanes in the North Atlantic give rise to growth in the eastern Pacific. Compared to that in the North Atlantic, the variation in storm frequency response to warming is even larger in the eastern Pacific with a standard deviation of 0.5 in the fractional changes among the simulations.

In comparison to the North Atlantic and the eastern Pacific basins, there is more agreement among the models on the sign of change in hurricane frequency in the western Pacific. A total of 9 out of the 10 models produce a significant reduction with only 1 model (GFDL CM2.1) generating a small increase (~8%). The largest decline is roughly –50% from the ECHAM5 model. The standard deviation in the fractional change of hurricane frequency in this basin is 0.16, roughly half of that in the North Atlantic.

The results for the northern Indian Ocean show much larger error bars, resulting from there being few storms (~2 hurricanes per year) and yet considerable year-to-year variability in this basin. Much longer integrations would be needed to obtain more stable statistics for this basin. Because of this, we will neglect further discussion of the results for the northern Indian Ocean.

For both the southern Indian and the South Pacific basins, none of the models produce a significant increase in hurricanes. Most of them generate a significant reduction with a few displaying small and insignificant changes. Despite this, the magnitude in reduction among the models still varies substantially with a standard deviation about 0.18 in the fractional change for both basins. This level of variation is similar to that in the western Pacific, but smaller than that in the North Atlantic and the eastern Pacific basins.

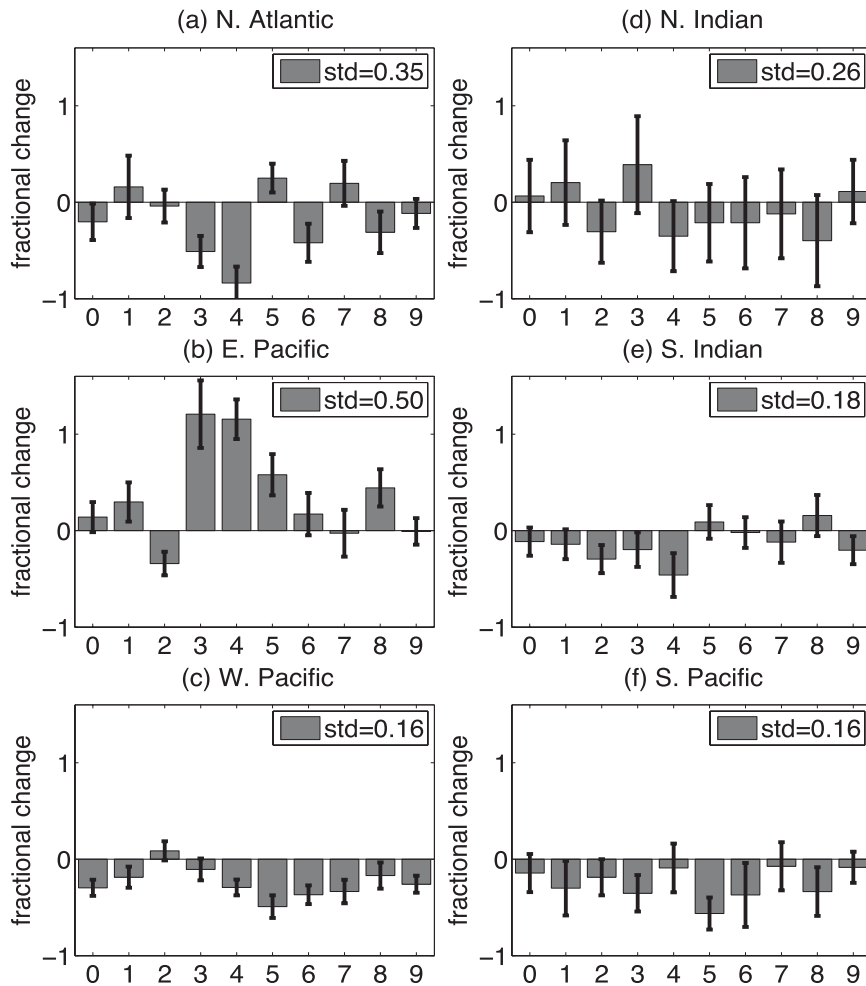


FIG. 1. Fractional changes in annual hurricane count for the (a) North Atlantic, (b) eastern Pacific, (c) western Pacific, (d) northern Indian, (e) southern Indian, and (f) South Pacific Oceans from 10 (0–9; see appendix A) SST warming experiments and the control experiment. Error bars show the 90% confidence interval; the legend shows the standard deviation of fractional changes across the models.

In general, the results in Fig. 1 reveal large uncertainties in future projections of the magnitude and (for some basins) even the sign of the response in basin-wide hurricane frequency, using a single atmospheric model. This large intermodel spread is entirely due to the differences in the projected SST warming anomaly since that is the only forcing parameter varying among the simulations. SST has long been recognized as important for storm genesis. Recent studies suggest that an index of relative SST [the SST in the tropical Atlantic's Main Development Region (MDR) minus the tropical mean SST] correlates well with the basin's storm activity and it is a more relevant quantity for controlling storm fluctuations in the North Atlantic than the local SST in isolation (Swanson 2008; Vecchi et al. 2008). Relative SSTs have also been utilized for hurricane seasonal forecast in

the North Atlantic (Zhao et al. 2010; Vecchi et al. 2011). The notion of relative SSTs has especially important implications in the projections of regional change of storm activities with global warming because both local North Atlantic and global mean SSTs are expected to rise substantially but the relative SST may or may not increase (Vecchi et al. 2008). Indeed, the results of recent TC-permitting high-resolution model simulations of North Atlantic storms support the notion that relative SST is a good predictor of twenty-first century TC projections (e.g., Knutson et al. 2008; ZHLV).

To what extent does this simple index of relative SST apply for other ocean basins? Physical arguments for relative SST emphasize its impact on the atmospheric instability and/or potential intensity (e.g., Vecchi and Soden 2007). This is because the atmospheric boundary

layer entropy is tied to local SST while the free tropospheric entropy is also strongly affected by remote ocean SSTs due to the small Coriolis force and the resulting weak temperature gradient in the tropical free troposphere (e.g., Sobel et al. 2002; Chiang and Sobel 2002). However, it is also well known that TC genesis depends sensitively on many other environmental factors such as the atmospheric vertical wind shear, middle troposphere moisture, and lower-level vorticity. It is not clear how these are affected by the spatial distribution of SSTs. Below we investigate the extent to which our simulated differences in hurricane frequency response may be explained by a simple relative SST index.

In the following analysis, we first compute monthly storm genesis frequency over each  $4 \times 5$  (latitude–longitude) grid box and obtain a climatological storm genesis function  $G(x, y, m)$  ( $x$  = longitude,  $y$  = latitude,  $m = 1, 12$ ) from the control simulation. To avoid an arbitrary choice for the temporal (months) and spatial (latitude–longitude) boundaries in the definition of an aggregated relative SST index (RSST) in each basin, we weight local RSST( $x, y, m$ ) (SST minus tropical mean SST) at each grid box ( $x, y$ ) by  $G(x, y, m)$  to obtain an annual mean and then we compute the index by a spatial average over all grid boxes where any TC genesis occurs within an ocean basin in the control simulation. The genesis weighting over the 12 months provides a simple and objective way of defining the index at the most relevant times of year.

Figure 2 shows scatterplots of the fractional changes in annual hurricane count versus changes in RSST for five ocean basins. In the North Atlantic, all model results fall close to a straight line, with a correlation coefficient of about 0.93 and a slope roughly  $120\% \text{ K}^{-1}$  (equivalent to  $7 \sim 8$  hurricanes per year per kelvin). The deep drop of hurricanes in the UK HADGEM1 model is associated with distinct decrease of RSST. Both the level of correlation and the slope of the linear regression are consistent with that in ZHLV (see their Fig. 16) where results of four SST warming anomaly experiments as well as the present-day (1981–2005) simulations are shown. In the east Pacific, all models except the GFDL-CM2.1 also collapse well along a straight line, with correlation coefficient of 0.85 over all models and a slope of roughly  $\sim 130\% \text{ K}^{-1}$  (equivalent to  $\sim 12$  hurricanes per year per kelvin). The sharp increase of eastern Pacific storms in the two Hadley Centre models is again well predicted by the distinct rise of RSST in the eastern Pacific. In both the North Atlantic and the eastern Pacific, the level of correlation and the slope of dependence on RSST are close to the observed values from interannual variability shown in Zhao et al. (2010) where the model is used to study hurricane seasonal forecasts. Note that the definition

of the relative SSTs in ZHLV and Zhao et al. (2010) are slightly different from the one generalized here so as to apply to all ocean basins.<sup>2</sup> Figure 2d shows that in the south Indian Ocean, there is also a high correlation ( $r = 0.9$ ) between the response of hurricane frequency and changes in relative SST. Linear regression yields a roughly similar slope to that in the North Atlantic and the eastern Pacific. Compared to the latter two basins, much of the reduced variance in storm response in the south Indian is due to the fact that the two Hadley Centre models are not so distinctive in changes of RSST in this basin.

While most (72%–86%) of the intermodel variance in the North Atlantic, the eastern Pacific, and the southern Indian can be explained by the simple index of RSST, an examination of the results in Figs. 2e,c reveals a lower correlation for the South Pacific ( $r = 0.69$ ), and the coefficient become insignificant (at 95% level) in the western Pacific. The lack of correlation between SST and storm frequency in the western Pacific is also seen in the observed historical records (e.g., Chan and Liu 2004). To understand why RSST does not work well in the western Pacific, we break down the western Pacific into three subbasins: the South China Sea (SCS;  $0^\circ$ – $30^\circ\text{N}$ ,  $100^\circ$ – $125^\circ\text{E}$ ), the MDR ( $0^\circ$ – $30^\circ\text{N}$ ,  $125^\circ$ – $160^\circ\text{E}$ ), and the eastern west Pacific (EWP;  $0^\circ$ – $30^\circ\text{N}$ ,  $160^\circ$ – $180^\circ$ ). The percentages of hurricane genesis frequency are 9%, 66%, and 25% for the SCS, MDR, and EWP regions, respectively, in the control simulation, which is close to the observations (8%, 72%, and 20%). We find significant correlation between the response of hurricane genesis frequency and the relative SST in the MDR region of the west Pacific ( $r = 0.65$ ). However, the storm frequency response in the SCS and EWP regions show little correlation with their respective relative SSTs.

Figure 3 shows the correlation map between each western Pacific subbasin's hurricane genesis frequency and local change in RSST throughout the tropics. While there is a clear positive correlation between storm genesis frequency in the western Pacific MDR region and the MDR-relative SST, this is not the case for the SCS region for which the correlation is negative for most of the region. In the EWP region storm genesis frequency is strongly positively correlated to the central and eastern Pacific–relative SST (instead of the EWP-relative SST), which is consistent with the eastward shift of the genesis location in western Pacific during the El Niño years seen

<sup>2</sup> In ZHLV and Zhao et al. (2010), we define relative SSTs as the MDR SSTs minus the tropical mean SST ( $30^\circ\text{S}$ – $30^\circ\text{N}$ ) over the August–September–October season. The MDR regions are ( $10^\circ$ – $25^\circ\text{N}$ ,  $80^\circ$ – $20^\circ\text{W}$ ) for the North Atlantic and ( $7.5^\circ$ – $15^\circ\text{N}$ ,  $160^\circ$ – $80^\circ\text{W}$ ) for the eastern Pacific.

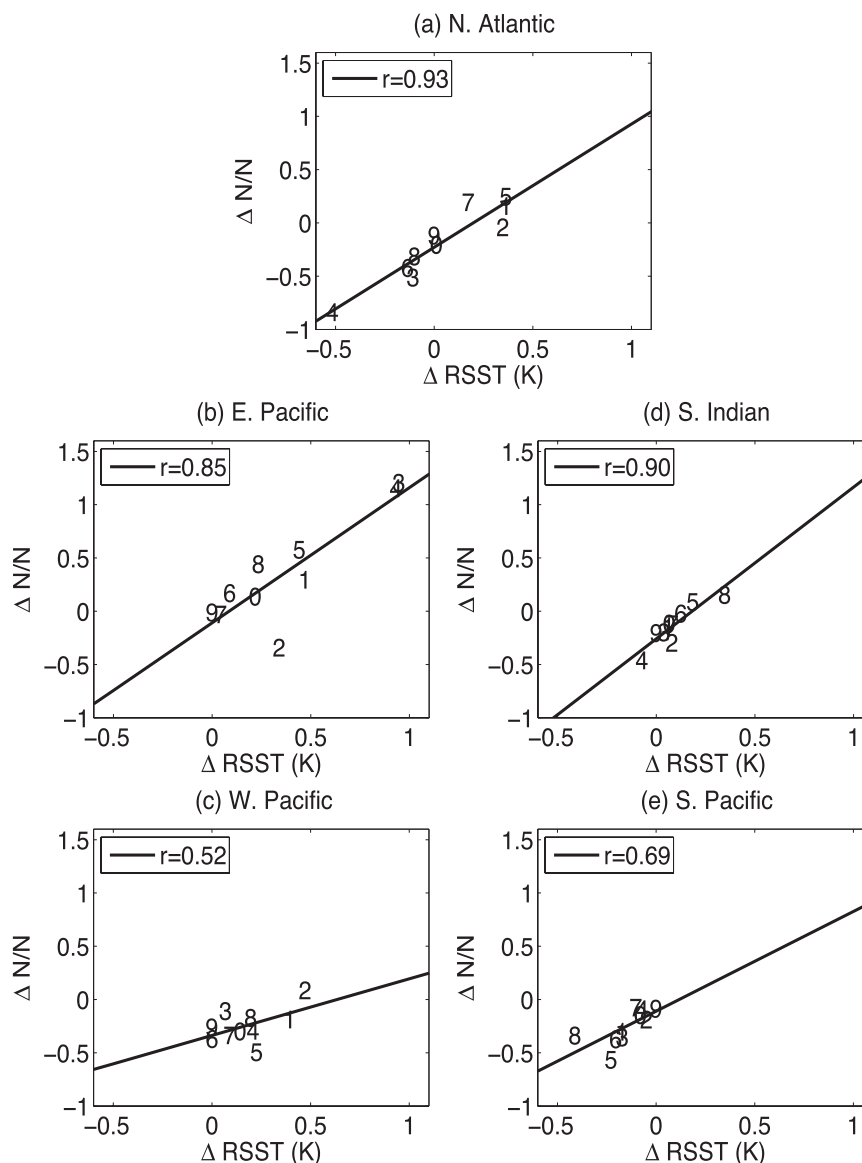


FIG. 2. Scatterplot of the fractional changes in annual hurricane count ( $\Delta N/N$ ) vs changes in a relative SST index (RSST, defined as a basin's storm development region SST minus tropical mean SST, see text for details) for the (a) North Atlantic, (b) eastern Pacific, (c) western Pacific, (d) southern Indian, and (e) South Pacific basins. Lines are linear regressions; the legend shows the correlation coefficient.

in the observational studies (e.g., Chia and Ropelewski 2002).

It is probably not surprising that such a simple relative SST index may not work well for every ocean basin given the fact that storm genesis is strongly affected by a variety of aspects of the atmospheric circulation, such as the monsoon in the SCS. In general, the tropical spatial distribution of SST affects the distribution of moist convective activity and associated large-scale atmospheric circulation, which strongly interact and

together determine the dynamical and thermodynamical structure as well as the transient activity of the tropical atmosphere. Below we explore which characteristics of the atmospheric properties control fluctuations of regional storm genesis frequency in this model.

### 3. Genesis parameters

Empirical parameters for TC genesis have been explored beginning with the work of Gray (1968) and more

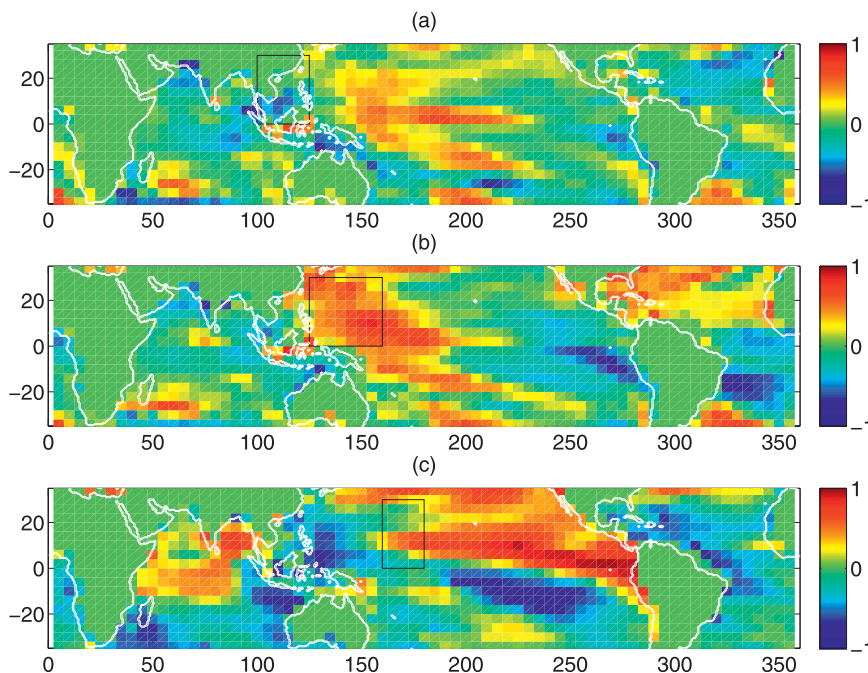


FIG. 3. Correlation maps between the local change in relative SST (warming minus control) and the change in hurricane genesis frequency from three subbasins in the western Pacific: (a) SCS, (b) MDR, and (c) EWP. Black boxes show the boundary of each region where storm genesis frequency is computed.

recently that of DeMaria et al. (2001), Emanuel and Nolan (2004), and others. TC genesis parameters have also been used to diagnose TC activities and possible future changes in coarse-resolution climate models (e.g., Royer et al. 1998; Camargo et al. 2007). Emanuel (2008) provided a short summary on a genesis potential index (GPI) that incorporates four environmental factors: potential intensity (Emanuel 1988), midlevel relative humidity, magnitude of the vector shear between the high- and low-level wind, and the lower-level absolute vorticity. In contrast to the magnitude of the vertical shear of vector wind, the vertical shear of zonal wind has also been suggested to be important for TC genesis through its impact on tropical synoptic-scale disturbance in the west Pacific (e.g., Li 2006; Li et al. 2010). Very recently, Held and Zhao (2011) demonstrated that an index for midlevel atmospheric vertical mass flux can be useful in understanding the global mean reductions of TC and hurricane frequency in their idealized climate change experiments.

Our purpose here is to investigate to what extent these parameters are useful in explaining our simulated differences in the response of basin-wide hurricane frequency for all ocean basins. In view of the above, our choice of the environmental parameters for each storm

genesis region includes: 1) potential intensity (PI),<sup>3</sup> 2) relative humidity at 600 hPa ( $RH_{600}$ ), 3) absolute vorticity at 850 hPa ( $\eta_{850}$ ), 4) the magnitude of the vertical shear ( $S$ ) of vector winds between 200 and 850 hPa, 5) vertical shear ( $S_z$ ) of zonal wind between 200 and 850 hPa ( $S_z = U_{200} - U_{850}$ , no absolute value taken), and 6) vertical pressure velocity ( $\omega_{500}$ ) at 500 hPa. All these indices are computed based on monthly mean fields following the same genesis weighting procedure described above for the calculation of relative SST index.

Figure 4 shows scatterplots of the fractional changes in annual hurricane count (ordinate) versus changes in each of the six indices (abscissa) for the five ocean basins with each column for one basin and with each row for one parameter (for easy comparison,  $-\Delta S$ ,  $-\Delta S_z$ , and  $-\Delta\omega_{500}$  are shown and the sign of  $\eta_{850}$  in the Southern Hemisphere basins is reversed). In the North Atlantic, the eastern Pacific, and the southern Indian basins, not only are the storm responses highly correlated to changes

<sup>3</sup> As in Held and Zhao (2011), the calculation follows Bister and Emanuel (2002), assuming a ratio of thermal to momentum drag coefficients of 0.5, assuming air parcel ascent between the pseudoadiabatic and adiabatic limits ( $SIG = 0.5$ ) and including storm dissipative heating.

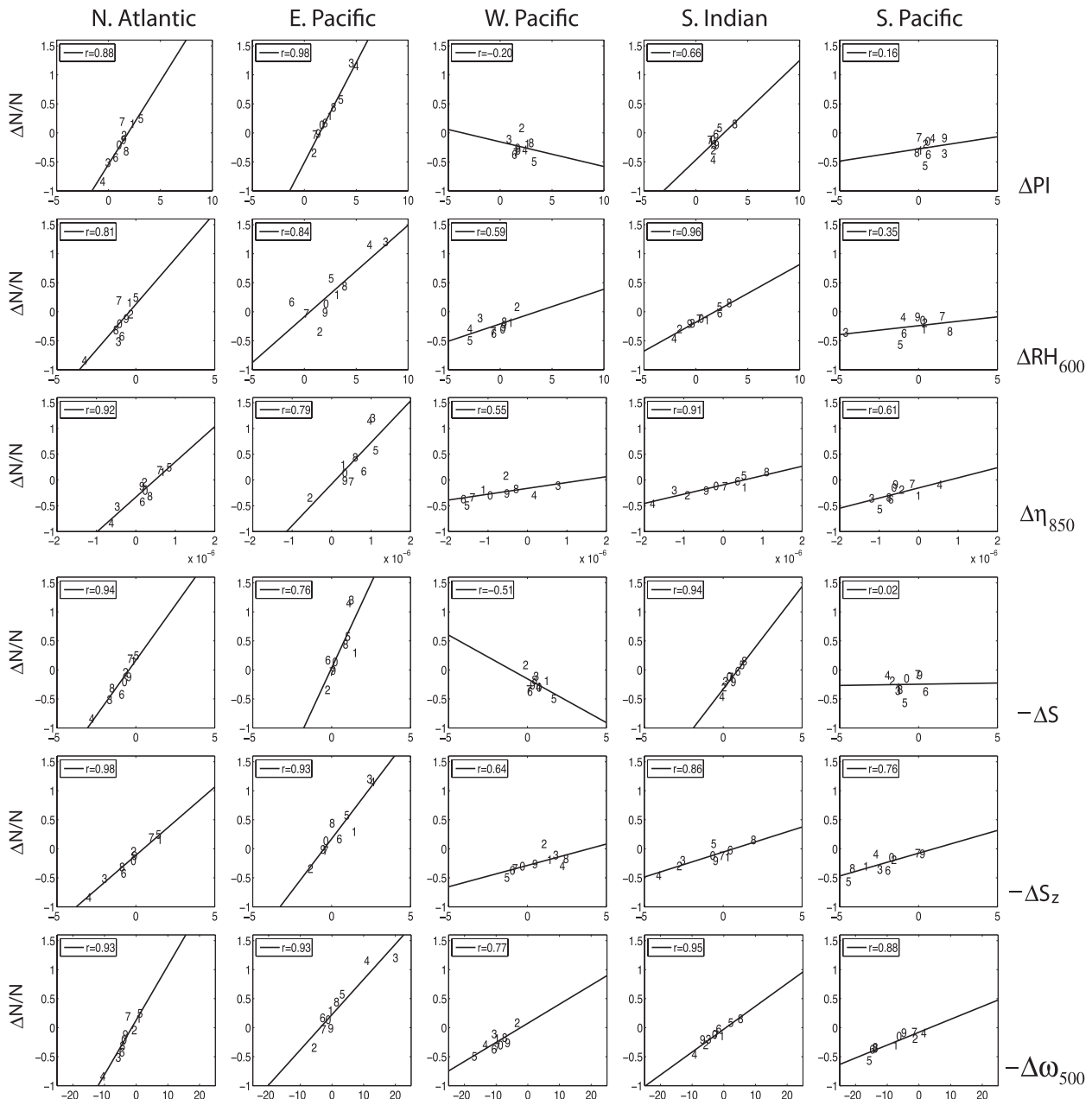


FIG. 4. Scatterplots of the fractional changes in annual hurricane count ( $\Delta N/N$ ; ordinate) vs changes in each of the six indices of atmospheric parameters (abscissa) for five ocean basins. (left to right) North Atlantic, eastern Pacific, western Pacific, southern Indian, and South Pacific. (top to bottom) Potential intensity ( $\Delta PI$ ;  $m s^{-1}$ ), 600-hPa relative humidity ( $\Delta RH_{600}$ ; %), 850-hPa vorticity ( $\Delta \eta_{850}$ ;  $1 s^{-1}$ ), magnitude of vertical shear of vector wind ( $-\Delta S$ ;  $m s^{-1}$ ) between 200 and 850 hPa, vertical shear of zonal wind ( $-\Delta S_z$ ;  $m s^{-1}$ ) between 200 and 850 hPa, and 500-hPa vertical pressure velocity ( $-\Delta \omega_{500}$ ;  $hPa day^{-1}$ ). The legend shows the correlation coefficient. The sign of  $\eta_{850}$  in the Southern Hemisphere basins is reversed.

in RSST (Figs. 2a,b,d), but they are also well correlated with each of the six atmospheric parameters, which are directly relevant for storm genesis. Further examinations reveal that these large-scale atmospheric environmental parameters are also mutually correlated and correlated with the relative SST in these basins (not shown).

However, the above is not true in the South Pacific and the western Pacific where we have seen the correlation between storm frequency and RSST is weaker (Figs. 2c,e). Except for  $\eta_{850}$  for the South Pacific and  $RH_{600}$  for the western Pacific both of which show only marginal correlation with the response of hurricanes, none of the

other parameters used in the GPI in Emanuel (2008) and many other previous studies display significant correlation in these two basins. In particular, the potential intensity (PI) and the vertical shear index ( $S$ ) fail to be indicators for the simulated storm differences in these basins. In contrast, the 500-hPa vertical pressure velocity ( $\omega_{500}$ ) and the vertical shear of zonal wind ( $S_z$ ) present a reasonably strong correlation ( $r = 0.64 - 0.88$ , see Fig. 4, bottom two panels). Moreover, these two indices also exhibit high correlation to the responses of storms in all other ocean basins. This result suggests a distinctive role of these two parameters in controlling and predicting storm frequency response in all ocean basins as the tropical atmospheric circulation changes with global warming. This result is also broadly consistent with Murakami et al. (2012) who studied future changes in TC activity by using a different AGCM with multi-physics and multi-SST ensemble experiments.

Table 2 provides a summary of the correlation coefficient between changes in annual hurricane frequency and changes in all seven (RSST and six atmospheric parameters) indices of storm environmental parameters for five ocean basins. Boldfaced coefficients denote significance at the 95% confidence level, assuming models are independent and normally distributed. We emphasize that all of the six atmospheric indices are determined by the SST anomaly fields used in these simulations. The fact that  $S_z$  and  $\omega_{500}$  are more highly correlated with the hurricane responses than RSST implies that there are better SST-based indices than RSST for explaining the model results.

#### 4. Geographical distribution of changes in hurricane genesis frequency

The aggregation of storm frequency over individual ocean basins as shown in section 2 is one natural way of analyzing the GCM simulated response in hurricane frequency. Figure 5 provides maps of geographical distribution of the changes in annual hurricane genesis frequency. Figure 5a shows the response averaged over the eight global warming experiments using the SST anomalies projected from individual coupled models. Regions where at least 6 out of the 8 (75%) models agree on the sign of change are stippled. To satisfy a sign change the absolute value of the change must be greater than  $0.05 \text{ yr}^{-1}$  per  $4^\circ \times 5^\circ$  area.

In the western Pacific, most models produce the largest reduction between  $135^\circ$  and  $165^\circ\text{E}$  where the control simulation generates the greatest climatological number of storms. Near the date line, there appears an eastward and poleward shift of storm genesis frequency leading to an increased activity in the central Pacific. In the eastern

TABLE 2. Correlation coefficients between changes in annual hurricane frequency and changes in each of the 7 environmental indices for the 5 ocean basins from the 10 global warming experiments. Boldfaced coefficients denote significance at the 95% confidence level.

Correlation	RSST	PI	RH <sub>600</sub>	$\eta_{850}$	$-S$	$-S_z$	$-\omega_{500}$
North Atlantic	<b>+0.93</b>	<b>+0.88</b>	<b>+0.81</b>	<b>+0.92</b>	<b>+0.94</b>	<b>+0.98</b>	<b>+0.93</b>
Eastern Pacific	<b>+0.85</b>	<b>+0.98</b>	<b>+0.84</b>	<b>+0.79</b>	<b>+0.76</b>	<b>+0.93</b>	<b>+0.93</b>
Western Pacific	+0.52	-0.20	<b>+0.59</b>	+0.55	-0.51	<b>+0.64</b>	<b>+0.77</b>
Southern Indian	<b>+0.90</b>	<b>+0.66</b>	<b>+0.96</b>	<b>+0.91</b>	<b>+0.94</b>	<b>+0.86</b>	<b>+0.95</b>
South Pacific	<b>+0.69</b>	+0.16	+0.35	<b>+0.61</b>	+0.02	<b>+0.76</b>	<b>+0.88</b>

Pacific, most models exhibit the sharpest rise of genesis activity off the west coast of central America at about  $245^\circ\text{E}$ . Overall the change in hurricane genesis frequency in the North Pacific Ocean may be described as a systematic basin-scale migration from the western to the central and eastern part of the ocean. The eastward movement of the Pacific tropical cyclone locations has also been noted in a recent study using a different global atmospheric model with 40-km mesh and the ECHAM5 SST warming anomaly (Li et al. 2010).

In the North Atlantic, there exists a similar pattern of basin-scale movement of hurricane activity with reductions in the western and southern part of the basin and a slight increase in the eastern and northern part of the basin although the magnitude of change is much smaller in the absolute number. However, the fraction change is comparable to that in the North Pacific (not shown). In the South Hemisphere, there is no evidence of such a basin-scale eastward migration of storm activity.

For comparison with the averaged responses from the 8 individual models, Fig. 5b also displays the result from the ENSEMBLE experiment, which uses the 18-model ensemble mean SST warming anomaly as the forcing. The results are broadly similar with both exhibiting similar magnitude basin-scale eastward movement of hurricane genesis frequency in the North Pacific and the North Atlantic. When zonally averaged, both results also display a small poleward shift of genesis frequency with an increase in activities poleward of roughly  $18^\circ(\text{N,S})$  and reductions equatorward (not shown). The largest zonally averaged reductions occur at  $12^\circ(\text{N and S})$ , where there exists maximum zonally averaged climatological genesis frequency in the control simulation. Globally, the averaged reduction in hurricane frequency across the eight warming experiments is about 10% with a standard deviation of 8%.

To understand the responses in hurricane genesis frequency in Fig. 5, we examine the spatial distribution of the changes in 500-hPa vertical pressure velocity,  $\Delta\omega_{500}$  between the warming and the control experiments in Fig. 6 ( $-\Delta\omega_{500}$  is shown for easy comparison with Fig. 5).

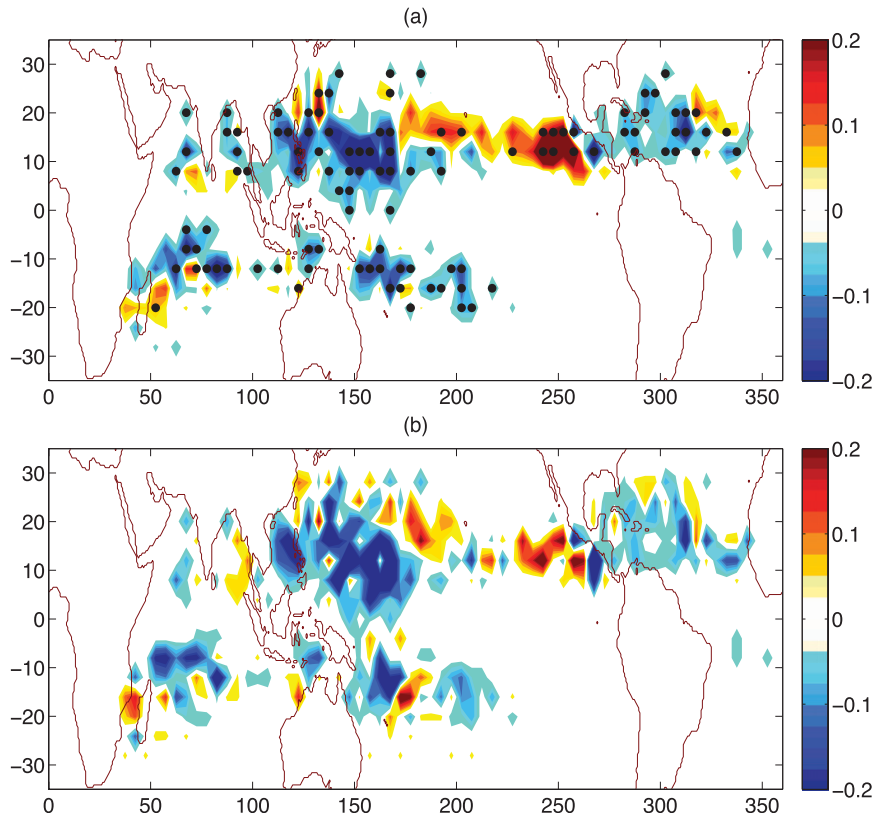


FIG. 5. (a) Geographical distribution of the changes in annual hurricane genesis frequency averaged from the eight global warming experiments [unit: number  $\text{yr}^{-1}$  per  $4^\circ \times 5^\circ$  (lat–lon)]. Stippled areas denote grid boxes where at least 6 out of the 8 (75%) models agree on the sign of change. (b) As in (a), but for changes from the ENSEMBLE (18-model ensemble mean SST anomaly) experiment.

Here  $\Delta\omega_{500}$  is defined as annual mean values weighted by monthly climatological TC genesis frequency at each  $4^\circ \times 5^\circ$  (latitude–longitude) grid box from the control simulation following the same procedure as described in section 2. Figure 6a shows that most SST anomaly patterns produce a distinct reduction in midtroposphere vertical ascent in the western Pacific and an increase in ascent in the central and eastern Pacific, consistent with a general slowdown of Walker circulation in the warmer climate (Vecchi et al. 2006). Regions of reduced (increased) midtropospheric vertical convective mass flux correspond reasonably well with reduced (increased) storm genesis activity in both the magnitude and the spatial distribution.

A similar pattern (although with much smaller magnitude) of basin-scale change in convective mass flux can also be discerned in the North Atlantic with a reduction in the western basin and less reduction or an increase in the eastern basin, once again consistent with the eastward movement of storm genesis activity in the North Atlantic. Finally, Fig. 6b confirms that the changes in

$\omega_{500}$  from the ENSEMBLE experiment are similar to the averaged results from the eight individual models. While an El Niño-like SST warming pattern may contribute to the change in seasonal-scale convective activity and the associated slowdown of tropical zonal overturning motion in the North Pacific and North Atlantic, the uniform 2-K warming experiment (P2K) also produces a similar change (not shown), suggesting that changes in convective activity and zonal circulation associated with uniform warming (e.g., Held and Soden 2006; Vecchi et al. 2006) may be the root cause of the basin-scale migration of storm genesis frequency.

## 5. Discussion and conclusions

We have utilized a TC-permitting GCM to investigate the hurricane frequency response to SST warming anomalies generated by coupled models for the late-twenty-first century using the Special Report on Emissions Scenarios (SRES) A1B scenario. We present the results for SST anomalies computed by averaging over 18 CMIP3 models

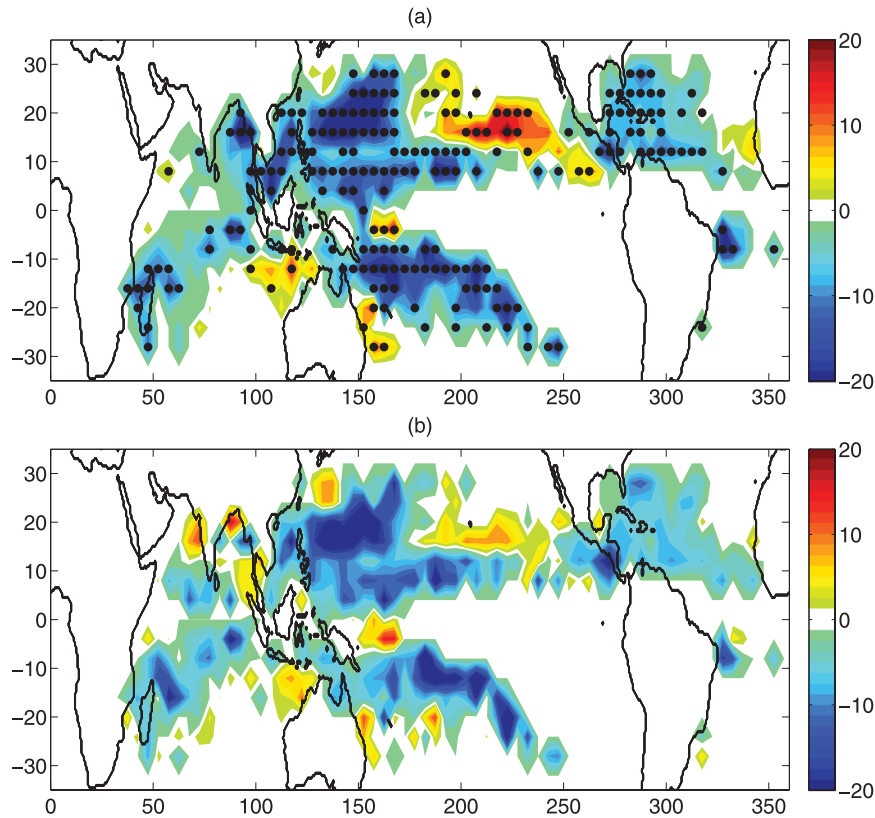


FIG. 6. (a) As in Fig. 5a, but for the changes in 500-hPa vertical pressure velocity ( $-\Delta\omega_{500}$ , hPa day $^{-1}$ ). The quantity  $\Delta\omega_{500}$  is defined as an annual mean weighted by monthly climatological TC genesis frequency at each  $4^\circ \times 5^\circ$  (lat–lon) grid box from the control simulation as described in section 2. (b) As in (a), but for the changes from the ENSEMBLE experiment.

as well as from individual realizations from 8 different models. In addition to these coupled model projections, we have also included a simple experiment with the control SST uniformly warmed by 2 K. In all cases, we also double the concentration of  $\text{CO}_2$  in the atmosphere, a change consistent to that imposed over the twenty-first century in the A1B experiments. This relatively large number of experiments makes it possible for us to systematically explore one aspect of the uncertainty in future projections of basin-wide hurricane activities that results from the variety of projections of the spatial pattern of tropical warming.

For each ocean basin, we find large intermodel spread in the magnitude and (for some basins) even the sign of the change in hurricane frequency among the different SST projections. The sizable intermodel variations are useful for exploring features of the SST warming pattern that are important for regional response of hurricane frequency. In the North Atlantic, the eastern Pacific, and the southern Indian basins, most (72%–86%) of the intermodel variance in storm frequency response can be explained by a simple relative SST index defined as a

basin's storm development region SST minus the tropical mean SST. The explained variance is significantly lower in the South Pacific (48%) and much lower in the western Pacific basin (27%). However, when the western Pacific is separated into three subbasins, 42% of the intermodel variance in its MDR can still be accounted for by the simple relative SST index, while storms in the South China Sea and the eastern west Pacific region correlate to the remote region SST in the central and eastern Pacific instead of their local relative SSTs. Despite this complexity in the western Pacific, for most ocean basins, the future projection of a basin's storm frequency using this time-slice approach depends largely on the projected relative warming of the basin with respect to the tropical mean ocean. Given the large divergence in regional SST projections, this result further emphasizes the importance in assessing and improving the quality of these projections in global climate models (e.g., Vecchi et al. 2008; Sugi et al. 2009).

To probe changes in tropical atmospheric circulation and thermodynamical properties relevant to storm genesis we have also explored six atmospheric parameters

which include four commonly used parameters [i.e., potential intensity (PI), 600-hPa relative humidity ( $RH_{600}$ ), 850-hPa absolute vorticity ( $\eta_{850}$ ), the magnitude of vertical shear of vector wind between 200 and 850 hPa ( $S$ )] as well as two not commonly used variables [the vertical shear of zonal wind between 200 and 850 hPa ( $S_z$ ) and 500-hPa vertical pressure velocity ( $\omega_{500}$ )]. In the North Atlantic, the eastern Pacific, and the southern Indian basins, where the storm responses are highly correlated to changes in relative SSTs, the simulated storm frequency is also well correlated with each of the six atmospheric parameters indicating that changes in atmospheric conditions directly relevant to the model's storm genesis are closely tied to the relative warming of these basins' SST with respect to tropical mean ocean warming.

However, in the South Pacific and the western Pacific, none of the four commonly used parameters display strong correlation to simulated storm frequency. In particular, the potential intensity (PI) and the magnitude of vertical shear ( $S$ ) fail entirely to be an indicator for the simulated differences in storm frequency in both basins. In contrast, 500-hPa vertical pressure velocity ( $\omega_{500}$ ) and the vertical shear ( $S_z$ ) of zonal wind between 200 and 850 hPa exhibit high correlation to changes of storm frequency in all ocean basins. Globally, in addition to a modest reduction of total hurricane frequency, the simulation results exhibit a small but robust eastward and poleward migration of genesis frequency in both the North Pacific and the North Atlantic Oceans upon warming. The eastward movement of hurricane genesis frequency is once again well correlated to changes in  $\omega_{500}$ , which displays a slowdown of the Walker circulation in warmer climate.

We emphasize that  $\omega_{500}$  measures tropical seasonal-scale overturning motion where vertical mass flux occurs primarily through convective clouds. An incorporation of a measure of convection into a TC genesis index was also proposed by Royer et al. (1998), where convective precipitation was directly used to replace the thermodynamical potential in Gray (1975). However, there are two components in the change of convective precipitation in the global warming experiments. One is associated with the increase of boundary layer humidity, which roughly follows the Clausius–Clapeyron scaling. The other is associated with the response in convective mass flux, which decreases globally (e.g., Held and Soden 2006). Our results herein together with Held and Zhao (2011) suggest that it is the vertical convective mass flux that plays a distinctive role in controlling and predicting the response in storm genesis frequency from the regional to the global scale as the tropical atmospheric circulation changes with global warming. A possible physical connection and a scaling argument between

convective mass fluxes and TC genesis has also been discussed in Held and Zhao (2011).

While a variety of twenty-first-century SST warming anomalies projected by individual coupled climate models have been explored in this study, our simulated hurricane responses are based on a single atmospheric model. The results remain to be further evaluated across different models. Nevertheless, our results are broadly consistent with recent studies that used different models that have explored the importance of SST warming pattern in future projections of storm activity (e.g., Chauvin and Royer 2010; Sugi et al. 2009). A multimodel intercomparison would be useful to explore the uncertainty resulted from the formulation of individual models' physics and dynamics. We emphasize that a model intercomparison must be pursued systematically under controlled conditions so as to isolate the effect from model differences from the differences in forcing and the storm detection and tracking algorithm. For example, Villarini et al. (2011) shows that some of the divergence in simulated North Atlantic storm frequency response among different models for apparently the same SST forcing (see Knutson et al. 2010 for a summary) are in fact due to the differences in SST forcing since they are extracted differently (some use linear trends; some use differencing between the last and the first 20-yr period of each simulation). This and other considerations complicate the direct comparison between our results and others (e.g., Emanuel et al. 2008; Sugi et al. 2009; Chauvin and Royer 2010).

Further, we emphasize that all of the future projections of hurricane statistics discussed here are based on the time-slice method in which SST warming anomalies derived from lower-resolution coupled climate models are used as the lower boundary conditions for a global high-resolution atmospheric model. Despite many years of application of this approach, some studies suggest its limitations for studying regional climate change in certain locations such as South Asia and the Indian Ocean (e.g., Douville 2005; Copesey et al. 2006). Future research will be needed to better understand these limitations and implications and develop new methods (e.g., Emanuel et al. 2008; Knutson et al. 2008) for downscaling the effect of climate change on hurricane statistics in some regions. Ultimately, fully coupled ocean–atmospheric models at fine spatial resolution with integrations over the centennial scale will provide the most convincing simulations.

*Acknowledgments.* We thank Gabriel Vecchi for providing the SST warming anomalies projected for the late-twenty-first century from the Intergovernmental Panel on Climate Change (IPCC) Fourth Assessment Report (AR4) coupled models. We are grateful for helpful

discussion on this topic from Gabriel Vecchi, Tom Knutson, and Steve Garner, and S.-J. Lin for his central role in the development of this model. The comments and suggestions from three anonymous reviewers helped improve the manuscript. We acknowledge the various IPCC modeling groups for providing their data, and the Program for Climate Model Diagnosis and Intercomparison (PCMDI) and the IPCC Data Archive at the Lawrence Livermore National Laboratory/Department of Energy (LLNL/DOE) for collecting, archiving, and making the data readily available. This research used resources of the National Center for Computational Sciences at Oak Ridge National Laboratory, which is supported by the Office of Science of the Department of Energy under Contract DE-AC05-00OR22725. An award of computer time was provided by the Innovative and Novel Computational Impact on Theory and Experiment Program. Ming Zhao was supported by Grant NA17RJ2612 from the National Oceanic and Atmospheric Administration, U.S. Department of Commerce. The findings are those of the authors and do not necessarily reflect the views of the National Oceanic and Atmospheric Administration, or the U.S. Department of Commerce.

## APPENDIX A

### A List of the Sea Surface Temperature Warming Anomalies Used in this Study

The following provides a list of twenty-first-century sea surface temperature warming anomalies projected by the coupled climate models, including their ID number, acronyms, and descriptions of the corresponding modeling groups.

- 0 ENSEMBLE: 18-Model Ensemble Mean
- 1 GFDL-CM2.0: Geophysical Fluid Dynamics Laboratory
- 2 GFDL-CM2.1: Geophysical Fluid Dynamics Laboratory
- 3 UK-HADCM3: Hadley Centre for Climate Prediction and Research/Met Office
- 4 UK-HADGEM1: Hadley Centre for Climate Prediction and Research/Met Office
- 5 ECHAM5: Max Planck Institute for Meteorology
- 6 CCCMA: Canadian Centre for Climate Modeling and Analysis
- 7 MRI-CGCM: Meteorological Research Institute of Japan
- 8 MIROC-HI: Center for Climate System Research and JAMSTEC
- 9 P2K: Uniform 2-K warming

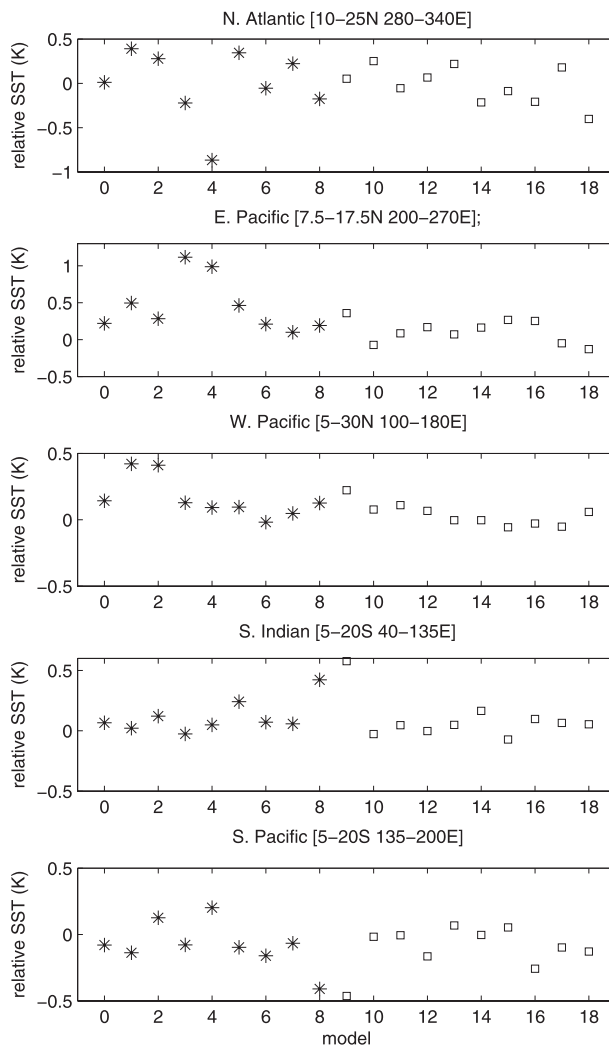


FIG. B1. A comparison of the variation in tropical cyclone MDR-relative SST warming anomalies among the 18-model ensemble mean and 8 selected models (stars: 0–8) with 10 other individual IPCC AR4 models (squares: 9–18). Relative SST warming anomalies are calculated from the August–September–October season for the Northern Hemisphere basins and from January–February–March season for the Southern Hemisphere basins.

## APPENDIX B

### Comparison of the Variation in Tropical Cyclone MDR-Relative SST Warming Anomalies among the 8 Selected Models and that for 10 Other IPCC AR4 Models

Figure B1 provides a comparison of the variation in tropical cyclone MDR-relative SST warming anomalies among the 18-model ensemble mean and 8 selected models (stars: 0–8) with 10 other individual IPCC AR4 models (squares: 9–18). In general, the eight selected

models are sufficient to represent the ensemble variations in the MDR-relative SST warming in both the North Atlantic and other ocean basins.

## REFERENCES

- Bengtsson, L., K. Hodges, M. Esch, North Keenlyside, L. Kornblueh, J.-J. Luo, and T. Yamagata, 2007: How may tropical cyclones change in a warmer climate. *Tellus*, **59A**, 539–561.
- Bister, M., and K. A. Emanuel, 2002: Low frequency variability of tropical cyclone potential intensity 1. Interannual to interdecadal variability. *J. Geophys. Res.*, **107**, 4801, doi:10.1029/2001JD000776.
- Bretherton, C. S., J. R. McCaa, and H. Grenier, 2004: A new parameterization for shallow cumulus convection and its application to marine subtropical cloud-topped boundary layers. Part I: Description and 1D results. *Mon. Wea. Rev.*, **132**, 864–882.
- Camargo, S., A. Sobel, A. G. Barnston, and K. Emanuel, 2007: Tropical cyclone genesis potential index in climate models. *Tellus*, **59A**, 428–443.
- Chan, J., and K. Liu, 2004: Global warming and western North Pacific typhoon activity from an observational perspective. *J. Climate*, **17**, 4590–4602.
- Chauvin, F., and J.-F. Royer, 2010: Role of the SST anomaly structures in response of cyclogenesis to global warming. *Hurricanes and Climate Change*, J. B. Elsner and T. H. Jagger, Eds., Springer, 39–52.
- , —, and M. Deque, 2006: Response of hurricane-type vortices to global warming as simulated by ARPEGE-CLIMAT at high resolution. *Climate Dyn.*, **27**, 377–399.
- Chia, H., and C. Ropelewski, 2002: The interannual variability in the genesis location of tropical cyclones in the northwest Pacific. *J. Climate*, **15**, 2934–2944.
- Chiang, J., and A. Sobel, 2002: Tropical tropospheric temperature variations caused by ENSO and their influence on the remote tropical climate. *J. Climate*, **15**, 2616–2631.
- Copsey, D., R. Sutton, and J. Knight, 2006: Recent trends in sea level pressure in the Indian Ocean region. *Geophys. Res. Lett.*, **33**, L19712, doi:10.1029/2006GL027175.
- DeMaria, M., J. Knaff, and B. H. Connell, 2001: A tropical cyclone genesis parameter for the tropical Atlantic. *Wea. Forecasting*, **16**, 219–233.
- Douville, H., 2005: Limitations of time-slice experiments for predicting regional climate change over South Asia. *Climate Dyn.*, **24**, 373–391.
- Dunkerton, T., M. Montgomery, and Z. Wang, 2009: Tropical cyclogenesis in a tropical wave critical layer: Easterly waves. *Atmos. Chem. Phys.*, **9**, 5587–5646.
- Emanuel, K., 1988: The maximum intensity of hurricanes. *J. Atmos. Sci.*, **45**, 1143–1155.
- , 2008: The hurricanes–climate connection. *Bull. Amer. Meteor. Soc.*, **89**, ES10–ES20.
- , and D. Nolan, 2004: Tropical cyclone activity and the global climate system. Preprints, *26th Conf. on Hurricanes and Tropical Meteorology*, Miami, FL, Amer. Meteor. Soc., 10A.2. [Available online at <http://ams.confex.com/ams/pdfpapers/75463.pdf>.]
- , R. Sundararajan, and J. Williams, 2008: Hurricanes and global warming: Results from downscaling IPCC AR4 simulations. *Bull. Amer. Meteor. Soc.*, **89**, 347–367.
- GFDL Global Atmospheric Model Development Team, 2004: The new GFDL global atmosphere and land model AM2–LM2: Evaluation with prescribed SST simulations. *J. Climate*, **17**, 4641–4673.
- Gray, W. M., 1968: Global view of the origin of tropical disturbances and storms. *Mon. Wea. Rev.*, **96**, 669–700.
- , 1975: Tropical cyclone genesis. Dept. of Atmospheric Science Paper 234, Colorado State University, Fort Collins, CO, 121 pp.
- Gualdi, S., E. Scoccimarro, and A. Navarra, 2008: Changes in tropical cyclone activity due to global warming: Results from a high-resolution coupled general circulation model. *J. Climate*, **21**, 5204–5228.
- Held, I. M., and B. J. Soden, 2006: Robust responses of the hydrological cycle to global warming. *J. Climate*, **19**, 5686–5699.
- , and M. Zhao, 2011: The response of tropical cyclone statistics to an increase in CO<sub>2</sub> with fixed sea surface temperatures. *J. Climate*, **24**, 5353–5364.
- Knapp, K. R., M. C. Kruk, D. H. Levinson, H. J. Diamond, and C. J. Neumann, 2010: The International Best Track Archive for Climate Stewardship (IBTrACS)—Unifying tropical cyclone data. *Bull. Amer. Meteor. Soc.*, **91**, 363–376.
- Knutson, T., J. Sirutis, S. Garner, G. Vecchi, and I. Held, 2008: Simulated reduction in Atlantic hurricane frequency under twenty-first-century warming conditions. *Nat. Geosci.*, **1**, 359–364, doi:10.1038/ngeo202.
- , and Coauthors, 2010: Tropical cyclones and climate change. *Nat. Geosci.*, **3**, 157–163, doi:10.1038/ngeo779.
- LaRow, T., Y.-K. Lim, D. Shin, E. Chassignet, and S. Cocks, 2008: Atlantic basin seasonal hurricane simulations. *J. Climate*, **21**, 3191–3206.
- Li, T., 2006: Origin of the summertime synoptic-scale wave train in the western North Pacific. *J. Atmos. Sci.*, **63**, 1093–1102.
- , M. Kwon, M. Zhao, J.-S. Kug, J.-J. Luo, and W. Yu, 2010: Global warming shifts Pacific tropical cyclone location. *Geophys. Res. Lett.*, **37**, L21804, doi:10.1029/2010GL045124.
- McDonald, R., D. Bleaken, D. Creswell, V. Pope, and C. Senior, 2005: Tropical storms: Representation and diagnosis in climate models and the impact of climate change. *Climate Dyn.*, **25**, 19–36.
- Meehl, G., C. Covey, T. Delworth, M. Latif, B. McAvaney, J. Mitchell, R. Stouffer, and K. Taylor, 2007: The WCRP CMIP3 multimodel dataset: A new era in climate change research. *Bull. Amer. Meteor. Soc.*, **88**, 1383–1394.
- Murakami, H., R. Mizuta, and E. Shindo, 2012: Future changes in tropical cyclone activity projected by multi-physics and multi-SST ensemble experiments using the 60-km-mesh MRI-AGCM. *Climate Dyn.*, doi:10.1007/s00382-011-1223-x, in press.
- Oouchi, K., J. Yoshimura, H. Yoshimura, R. Mizuta, S. Kusunoki, and A. Noda, 2006: Tropical cyclone climatology in a global-warming climate as simulated in a 20 km mesh global atmospheric model: Frequency and wind intensity analysis. *J. Meteor. Soc. Japan*, **84**, 259–276.
- Putman, W. M., and S.-J. Lin, 2007: Finite-volume transport on various cubed-sphere grids. *J. Comput. Phys.*, **227**, 55–78.
- Rayner, R., D. Parker, E. Horton, C. Folland, L. Alexander, D. Rowel, E. Kent, and A. Kaplan, 2003: Global analyses of sea surface temperature, sea ice, and night marine air temperature since the late nineteenth century. *J. Geophys. Res.*, **108**, 4407, doi:10.1029/2002JD002670.
- Royer, J.-F., F. Chauvin, B. Timbal, P. Araspin, and D. Grimal, 1998: A GCM study of the impact of greenhouse gas increase on the frequency of occurrence of tropical cyclones. *Climatic Change*, **38**, 307–343.

- Sobel, A., I. Held, and C. Bretherton, 2002: The ENSO signal in tropospheric temperature. *J. Climate*, **15**, 2702–2706.
- Sugi, M., A. Noda, and North Sato, 2002: Influence of the global warming on tropical cyclone climatology: An experiment with the JMA global model. *J. Meteor. Soc. Japan*, **80**, 249–272.
- , H. Murakami, and J. Yoshimura, 2009: A reduction in global tropical cyclone frequency due to global warming. *SOLA*, **5**, 164–167.
- Swanson, K. L., 2008: Nonlocality of Atlantic tropical cyclone intensities. *Geochem. Geophys. Geosyst.*, **9**, Q04V01, doi:10.1029/2007GC001844.
- Vecchi, G. A., and B. J. Soden, 2007: Effect of remote sea surface temperature change on tropical cyclone potential intensity. *Nature*, **450**, 1066–1071, doi:10.1038/nature06423.
- , —, A. T. Wittenberg, I. M. Held, A. Leetmaa, and M. J. Harrison, 2006: Weakening of tropical Pacific atmospheric circulation due to anthropogenic forcing. *Nature*, **441**, 73–76.
- , K. L. Swanson, and B. J. Soden, 2008: Whither hurricane activity? *Science*, **322**, 687–689.
- , M. Zhao, H. Wang, G. Villarini, A. Rosati, A. Kumar, I. M. Held, and R. Gudgel, 2011: Statistical-dynamical predictions of seasonal North Atlantic hurricane activity. *Mon. Wea. Rev.*, **139**, 1070–1082.
- Villarini, G., G. A. Vecchi, T. R. Knutson, M. Zhao, and J. A. Smith, 2011: North Atlantic tropical storm frequency response to anthropogenic forcing: Projections and sources of uncertainty. *J. Climate*, **24**, 3224–3238.
- Yoshimura, J., and M. Sugi, 2005: Tropical cyclone climatology in a high-resolution AGCM—Impacts of SST warming and CO<sub>2</sub> increase. *SOLA*, **1**, 133–136.
- , —, and A. Noda, 2006: Influence of greenhouse warming on tropical cyclone frequency. *J. Meteor. Soc. Japan*, **84**, 405–428.
- Zhao, M., and I. M. Held, 2010: An analysis of the effect of global warming on the intensity of Atlantic hurricanes using a GCM with statistical refinement. *J. Climate*, **23**, 6382–6393.
- , —, S.-J. Lin, and G. A. Vecchi, 2009: Simulations of global hurricane climatology, interannual variability, and response to global warming using a 50-km resolution GCM. *J. Climate*, **22**, 6653–6678.
- , —, and G. A. Vecchi, 2010: Retrospective forecasts of the hurricane season using a global atmospheric model assuming persistence of SST anomalies. *Mon. Wea. Rev.*, **138**, 3858–3868.